

光学学报

TIE 和角谱迭代用于光学元件表面划痕深度检测

孟昕¹, 王红军^{1*}, 王大森², 田爱玲¹, 刘丙才¹, 朱学亮¹, 刘卫国¹

¹ 西安工业大学陕西省薄膜技术与光学检测重点实验室, 陕西 西安 710021;

² 中国兵器科学院宁波分院, 浙江 宁波 310022

摘要 针对散射法在检测光学元件表面划痕时只能得到其光场分布而无法直接得到划痕深度信息的问题, 将角谱迭代算法、光强传输方程(TIE)和角谱迭代结合的算法应用到光学元件表面划痕深度检测中。首先, 采集光学元件表面的光场分布, 分别利用两种重建算法得到表面划痕的相位分布, 通过表面划痕对相位的调制特性计算出划痕深度; 然后, 从强度误差、相关系数及相对均方根误差来对两种算法的有效性进行评价; 最后, 通过实验验证了光学元件表面划痕深度重建结果的准确性。结果表明, 与角谱迭代算法相比, TIE 和角谱迭代相结合的算法重建划痕深度的相对误差更小, 重建效果更好, 重建精度更高。

关键词 测量; 散射法; 散射分布; 划痕深度; 相位重建; 角谱迭代算法; 光强传输方程

中图分类号 O436 文献标志码 A

DOI: 10.3788/AOS230499

1 引言

在各种各样的光学仪器中, 几乎都会用到光学元件^[1]。由光学元件表面划痕产生的散射光会增大系统噪声, 降低对比度等, 对整个光学系统的性能和正常运行造成影响。因此, 对光学元件表面划痕的检测非常重要^[2-4]。

光散射法作为一种非接触、快速、可靠的高分辨率检测方法, 在元件表面划痕检测领域的应用越来越广泛^[5-7]。在已有的表面划痕检测方法中, 只能通过 CCD 或 CMOS 接收经划痕散射后形成的光场分布, 而无法直接得出划痕的深度信息。划痕的深度、形状等高达 80% 的表面信息由相位信息表征^[8-10], 但在现有的光学设备采集过程中, 相位信息难以获得。因此, 相位重建技术对元件表面划痕深度检测具有重要意义^[11-13]。

目前, 迭代法和光强传输方程(TIE)法是两类典型的非干涉相位重建算法。迭代法中的经典 Gerchberg-Saxton(GS) 算法最早由 Gerchberg 和 Saxton^[14]提出, 之后相继出现杨-顾算法^[15]、混合输入输出算法(HIO)^[16]、角谱迭代算法、GS-TIE 算法等改进算法。TIE 算法最早由 Teague 提出^[17], 其将物平面上波的强度信息和相位信息与传播方向上的强度变化率联系起来, 将未知的相位变化转化成可见的强度变化, 从而求解物平面的相位信息。

2013 年, 刘宏展等^[18]基于角谱传播理论, 在传统

GS 迭代算法的基础上提出一种幅度梯度加成迭代算法, 为复杂光场的相位重建提供了一种新的方法。同年, 梁丽等^[19]在 GS 算法中引入 TIE 法和加速角谱迭代算法, 提出一种基于 TIE 的加速角谱迭代算法, 实现了更加精准快速的相位重建。2014 年, 程鸿等^[20]使用 TIE 和角谱迭代融合提出了适用于自然场景透镜模型的相位检索方法。2019 年, 孟春丽等^[21]利用 TIE 和角谱迭代算法, 基于三面光强分布实现了像面附近的彩色图像再现。2020 年, 于颖等^[22]结合 TIE 和 GS 算法实现了生物细胞彩色图像高分辨率相位重建。

针对光学元件表面划痕深度检测, 本文将角谱迭代算法、TIE+角谱迭代算法应用到光学元件表面划痕检测中。首先, 仿真得到光学元件表面的光场分布, 通过三维重建算法得到元件表面划痕的相位信息, 并根据表面划痕对相位的调制特性, 得到表面划痕的深度信息; 然后, 分别从强度误差、相关程度以及相对均方根误差来对两种重建算法的重建效果、精确度进行评价; 最后, 通过实验验证光学元件表面划痕深度重建结果的准确性。

2 基本原理

2.1 散射法检测原理

光学元件表面划痕的散射法检测原理如图 1 所示。激光器发出的光束经扩束准直后到达光学元件表面, 通过表面划痕的调制, 形成携带表面划痕深度信息

收稿日期: 2023-02-03; 修回日期: 2023-03-13; 录用日期: 2023-04-03; 网络首发日期: 2023-05-08

基金项目: 陕西省科技厅项目(2022JM-345)、陕西省教育厅项目(21JY019)

通信作者: *whj0253@sina.com

的光场分布,经传输之后由相机接收散射光场的强度分布。

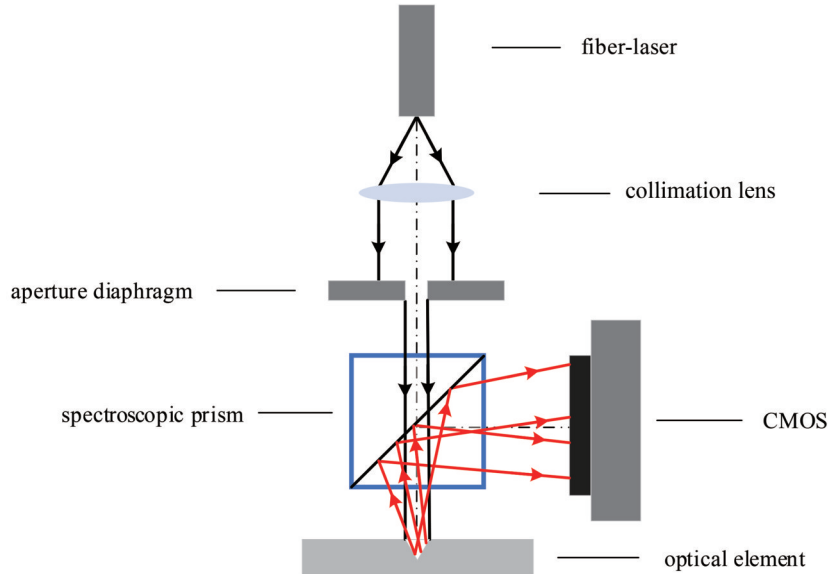


图1 散射法检测原理图
Fig. 1 Schematic of scattering method

2.2 角谱迭代算法

在直角坐标系中,令光学元件表面坐标为 (x_i, y_i) ,其光场振幅为 $U_i(x_i, y_i)$,相位分布为 $\varphi_i(x_i, y_i)$;在空间传播距离 z 后,到达CMOS接收面的坐标为 (x_o, y_o) ,

其光场振幅为 $U_o(x_o, y_o)$,相位分布为 $\varphi_o(x_o, y_o)$,元件表面、CMOS接收面的光场分布分别为 E_i 、 E_o 。由元件表面光场得到的CMOS接收面光场的角谱变换积分为

$$E_o(x_o, y_o) = \mathcal{F}^{-1} \left\{ \mathcal{F} \left\{ U_i(x_i, y_i) \exp[j\varphi_i(x_i, y_i)] \right\} \times H(f_x, f_y) \right\} = \mathcal{F}^{-1} \left\{ \mathcal{F} [E_i(x_i, y_i)] H(f_x, f_y) \right\}, \quad (1)$$

式中: j 为虚数单位; \mathcal{F} 、 \mathcal{F}^{-1} 分别表示傅里叶变换和傅里叶逆变换; f_x, f_y 为频域坐标; $H(f_x, f_y)$ 为空间频率传递函数。

角谱逆运算的表达式为

$$E_i(x_i, y_i) = \mathcal{F}^{-1} \left\{ \mathcal{F} [E_o(x_o, y_o)] H^*(f_x, f_y) \right\}, \quad (2)$$

式中: $H^*(f_x, f_y)$ 为 $H(f_x, f_y)$ 的共轭。 $H(f_x, f_y)$ 的表达式为

$$H(f_x, f_y) = \exp \left[jkz \sqrt{1 - (\lambda f_x)^2 - (\lambda f_y)^2} \right], \quad (3)$$

$$f_x = \frac{m}{\Delta L_h}, f_y = \frac{n}{\Delta L_h} \quad (m, n = -N/2, N/2 + 1, \dots, N/2 - 1), \quad (4)$$

式中: $k = 2\pi/\lambda$, λ 为光波长; ΔL_h 为CMOS接收面光场的计算宽度; m, n 均为采样点数; N 为采样点总数。

假设光学元件表面和CMOS接收面之间光场变换关系服从标量衍射理论,根据平面角谱传播理论,利用角谱传递函数可以构建光学元件表面和CMOS接收面之间的正向和逆向传播过程^[23],其主要思想就是选取随机相位作为CMOS接收面的初始相位,在两个面之间反复迭代,用实际所测强度值代替计算值,直到

误差达到预先设定的精度或者迭代次数达到设定的最大迭代次数为止。角谱迭代算法的基本迭代流程如图2所示。

迭代基本流程如下:1)选取CMOS接收面初始相位为随机相位 $\varphi_o(x_o, y_o)$;2)结合输入的散射强度分布 $I_o(x_o, y_o)$,振幅表示为 $U_o(x_o, y_o) = \sqrt{I_o(x_o, y_o)}$,得到CMOS接收面的光场分布 $E_o(x_o, y_o)$;3)利用式(2)进行变换得到光学元件表面光场 $E_i(x_i, y_i)$;4)提取并保留 $E_i(x_i, y_i)$ 的相位信息,将其振幅用单位振幅1代替,得到新的光学元件表面光场 $E'_i(x_i, y_i)$;5)利用式(1)对 $E_i(x_i, y_i)$ 进行角谱变换,得到新的CMOS接收面光场 $E'_o(x_o, y_o)$;6)提取CMOS接收面光场 $E'_o(x_o, y_o)$ 的当次迭代振幅信息;7)提取并保留 $E'_o(x_o, y_o)$ 的相位信息,将其振幅用实际所测振幅 $U_o(x_o, y_o)$ 代替,得到新的CMOS接收面光场 $E_o(x_o, y_o)$;8)设置迭代次数 S ,重复步骤2)~7),当迭代次数 s 达到设置的 S 时,迭代终止,这时再将CMOS接收面光场 $E_o(x_o, y_o)$ 进行角谱逆运算,得到光学元件表面的相位分布 $\varphi_i(x_i, y_i)$,其

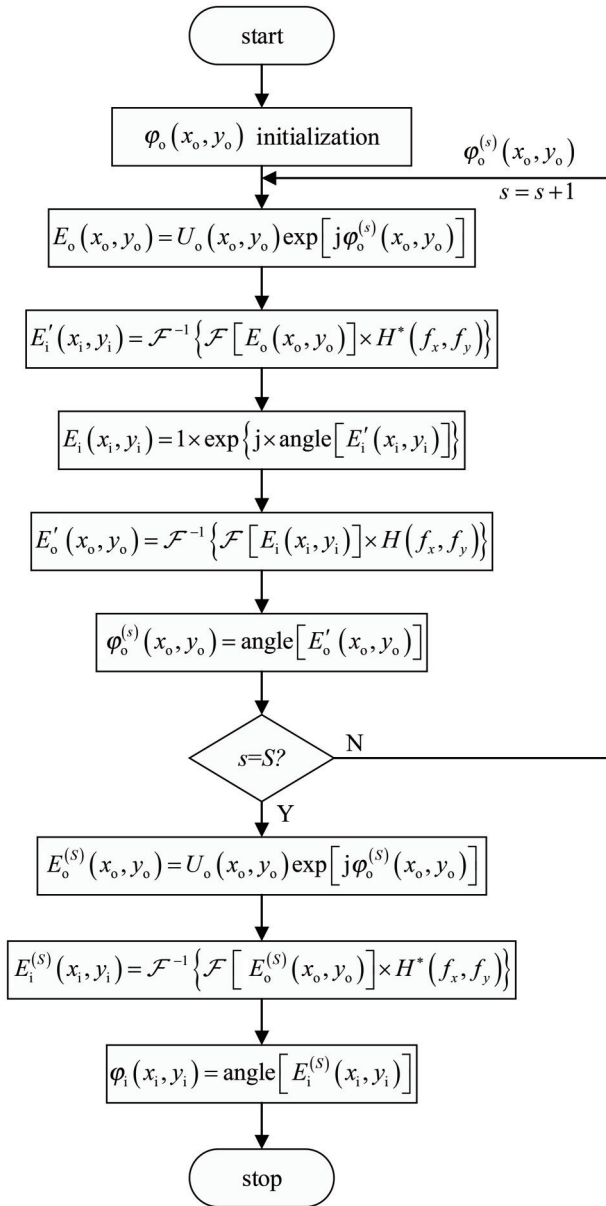


图2 角谱迭代算法流程

Fig. 2 Flow chart of angular spectrum iterative algorithm

中 $\text{angle}(\cdot)$ 为提取相位的函数。

根据光学元件表面划痕对相位的调制特性,通过式(5)可计算得到表面划痕的深度信息 $h(x_i, y_i)$:

$$h(x_i, y_i) = \frac{\lambda}{4\pi} \varphi_i(x_i, y_i)。 \quad (5)$$

2.3 TIE+角谱迭代算法

文献[19]与文献[20]将TIE与角谱迭代相结合实现了物面相位重建,本文基于文献[24]提出的对TIE的简单求解中的简单TIE(STIE)方法计算出CMOS接收面的相位分布,再结合角谱迭代算法进行表面划痕深度重建。

TIE方法的计算公式^[25]为

$$\nabla [I(x, y, z) \nabla \varphi(x, y, z)] = -\frac{2\pi}{\lambda} \frac{\partial I(x, y, z)}{\partial z}, \quad (6)$$

式中: I 为光强; φ 表示相位; z 方向为光轴方向; ∇ 表示垂直于 z 方向的 xoy 平面的微分算子。令 $E = \sqrt{I} \exp(j\varphi) = U \exp(j\varphi)$ 表示光场复振幅, $U = \sqrt{I}$ 表示振幅。

将TIE应用到光学元件表面划痕深度检测中,假设光强在垂轴方向近似均匀分布,令式(6)左端的光强 I 近似为常数 I_0 , TIE方法可以演变为STIE法^[24],计算方程为

$$I_0 \nabla^2 \varphi = -\frac{2\pi}{\lambda} \frac{\partial}{\partial z} I。 \quad (7)$$

对式(7)两边进行傅里叶变换并利用导数傅里叶变换性质 $\mathcal{F}[f^{(n)}] = (-jk_{\perp})^n \mathcal{F}(f)$, 得到

$$I_0 k_{\perp}^2 \mathcal{F}[\varphi(x, y)] = \mathcal{F}(V_{\text{Temp}}), \quad (8)$$

$$V_{\text{Temp}} = \frac{2\pi}{\lambda} \frac{\partial}{\partial z} I \approx \frac{2\pi}{\lambda} \frac{I_i - I_o}{z}, \quad (9)$$

式中: I_i, I_o 分别表示光学元件表面光强分布与CMOS接收面光强分布; z 表示两个面的距离; $k_{\perp} = \sqrt{k_x^2 + k_y^2}$ 表示空间角频率矢量(k_x, k_y)的模长。

利用STIE法计算求解即可得到CMOS接收面的相位分布,即

$$\varphi_{\text{TIE}}(x_o, y_o) = I_0^{-1} \mathcal{F}^{-1}[k_{\perp}^{-2} \mathcal{F}(V_{\text{Temp}})], \quad (10)$$

式中: $\mathcal{F}, \mathcal{F}^{-1}$ 表示二维傅里叶变换与傅里叶逆变换。TIE法计算CMOS接收面相位的流程如图3所示。

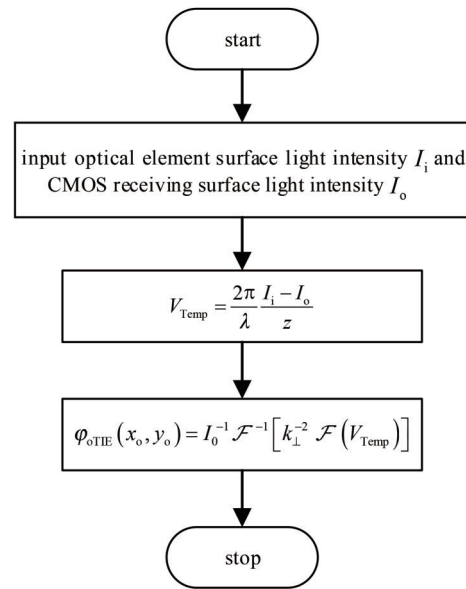


图3 TIE算法流程图

Fig. 3 Flow chart of TIE algorithm

TIE+角谱迭代算法重建表面划痕深度的基本流程与角谱迭代算法相同,只需要将初始相位 $\varphi_o(x_o, y_o)$ 改成TIE计算得出的相位 $\varphi_{\text{TIE}}(x_o, y_o)$ 即可,重建表面划痕相位后再通过式(5)计算出表面划痕的深度。

3 仿真与结果分析

本文将两种三维重建算法运用到光学元件表面划痕深度检测中。首先,模拟光学元件表面划痕分布及其散射光场分布;然后,对散射光场进行处理,重建表面划痕的相位信息;最后,计算得到表面划痕的深度信息。

3.1 仿真分析

首先,进行仿真计算,模拟光学元件表面散射光场

的生成过程。具体参数如下:波长 $\lambda=520\text{ nm}$,传播距离 $z=300\text{ mm}$,采样数 $M\times N=1280\times 1024$ 。仿真了光学元件表面深度均为43 nm的不同类型划痕,包括方形划痕、三角形划痕、椭圆形划痕。方形划痕表示上表面为方形、截面为方形的光学元件表面划痕,三角形划痕表示上表面为方形、截面为三角形的光学元件表面划痕,椭圆形划痕表示上表面为方形、截面为半椭圆形状的光学元件表面划痕。光学元件表面不同类型划痕的分布如图4所示。

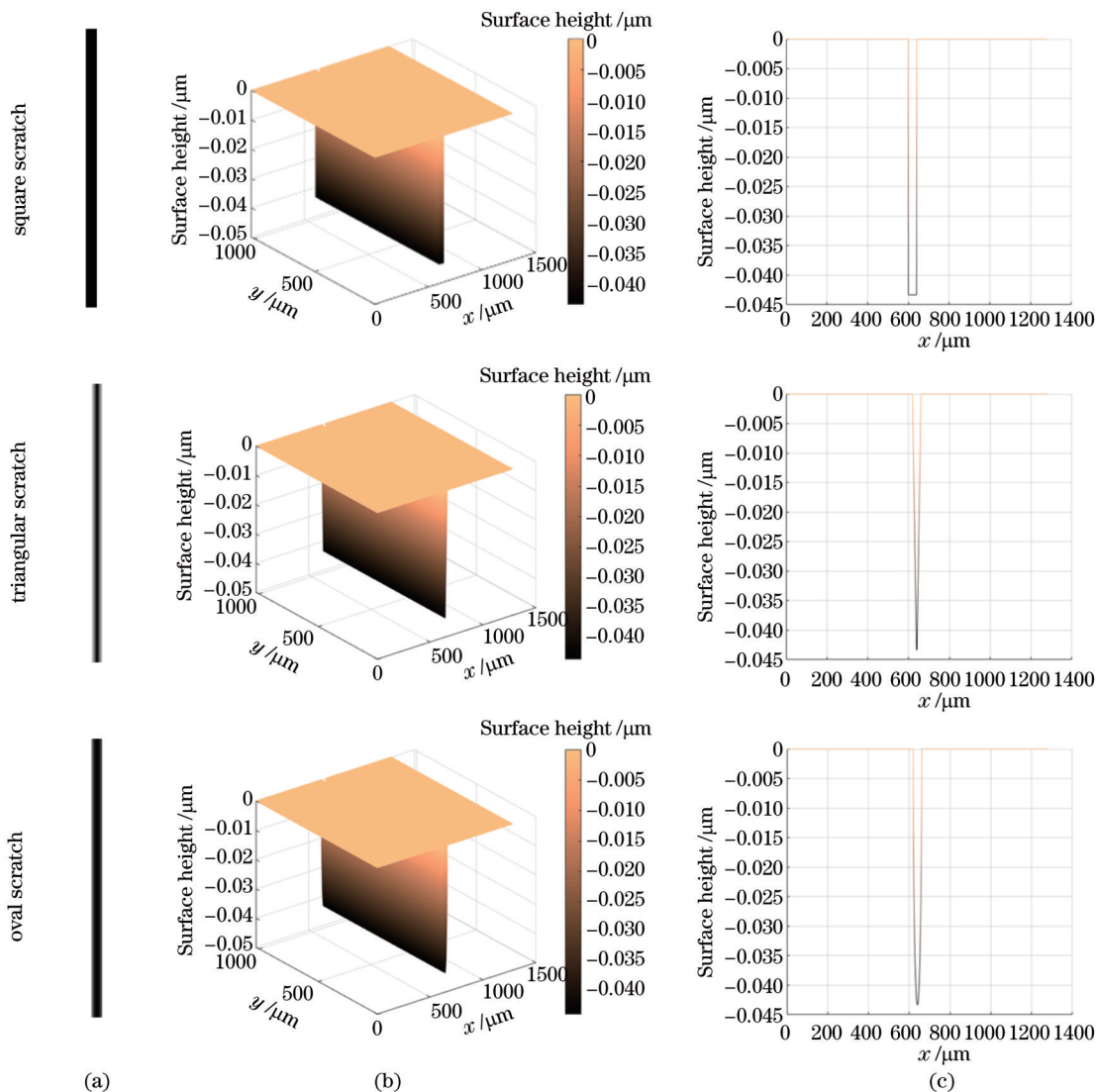


图4 光学元件表面划痕分布。(a)横向截面分布;(b)三维分布;(c)纵向截面分布

Fig. 4 Scratch distribution on the surface of optical components. (a) Transverse cross-section distribution; (b) three-dimensional distribution; (c) longitudinal cross-section distribution

然后,依据建立的光学元件表面与CMOS接收面传播关系模型,模拟光学元件表面散射光场的生成过程,得到方形划痕、三角形划痕、椭圆形划痕的散射光场分布,如图5所示。

最后,将划痕散射分布作为角谱迭代算法和TIE+角谱迭代算法的初始输入来重建划痕的相位分布,再通过式(5)计算表面划痕的深度。角谱迭代算法

的划痕深度重建结果如图6所示。TIE+角谱迭代算法的划痕深度重建结果如图7所示。

3.2 算法评价

为更好地衡量表面划痕深度重建结果是否准确,两种重建算法是否合理可靠,分别从强度误差、相关程度以及相对均方根误差来对两种重建算法的重建效果、精确度进行评价。

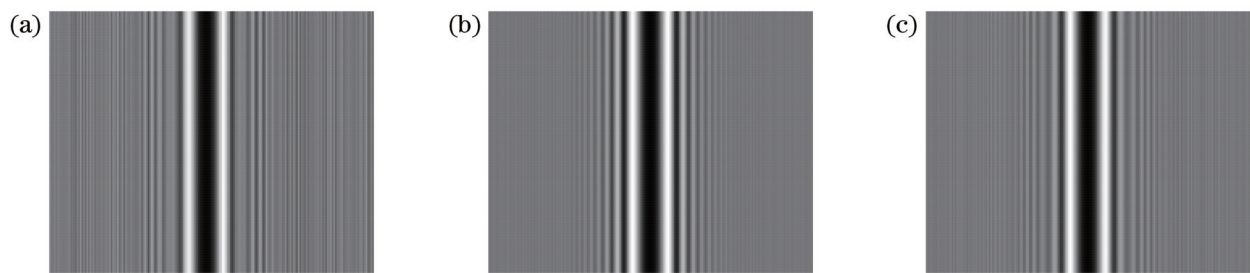


图5 不同类型划痕的散射光场分布。(a)方形划痕;(b)三角形划痕;(c)椭圆形划痕

Fig. 5 Scattered light field distribution of different types of scratches. (a) Square scratch; (b) triangular scratch; (c) oval scratch

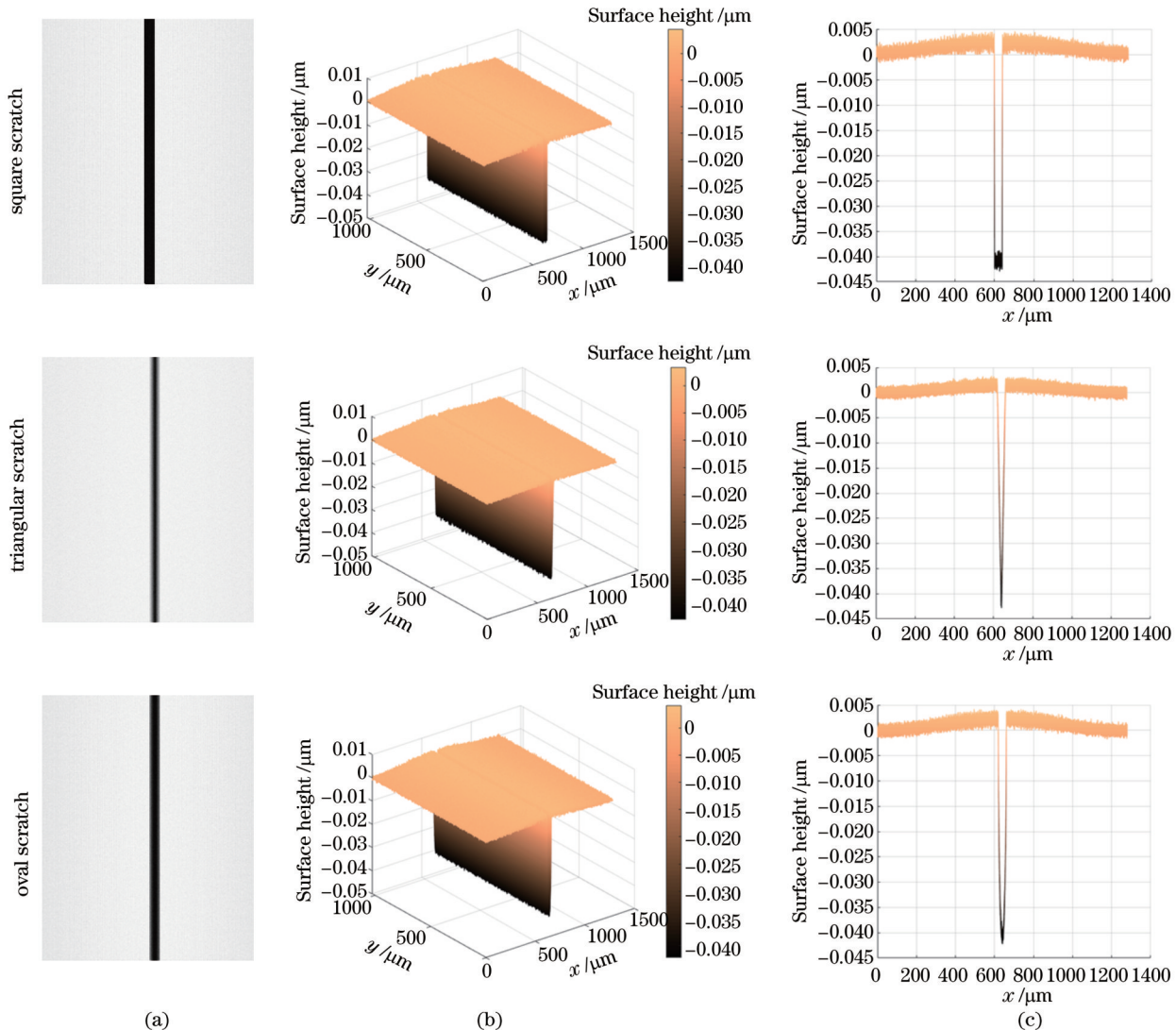


图6 角谱迭代算法重建结果。(a)横向截面分布;(b)三维分布;(c)纵向截面分布

Fig. 6 Reconstruction results of angular spectrum iterative algorithm. (a) Transverse cross-section distribution; (b) three-dimensional distribution; (c) longitudinal cross-section distribution

1)强度误差评价

首先,令每次迭代的散射分布强度计算值为 I_s ,真实强度值为 I_0 ,则该次迭代强度误差 E_{ss} 描述为 $E_{ss}=\frac{\sum(I_s-I_0)^2}{\sum I_0^2}$,对应的强度误差曲线如图8所示。

从图8可以看出,随着迭代次数的增加,强度误差

不断减小。设定 $S=5000$ 时,TIE+角谱迭代算法的强度误差小于角谱迭代算法;设定强度误差 $E_{ss}=5\times 10^{-7}$ 时,两种算法所需的迭代次数见表1,当达到设定的强度误差时,TIE+角谱迭代算法所需的迭代次数少于角谱迭代算法。可见,在收敛速度、相位重建精确度方面,TIE+角谱迭代算法均优于角谱迭代算法。

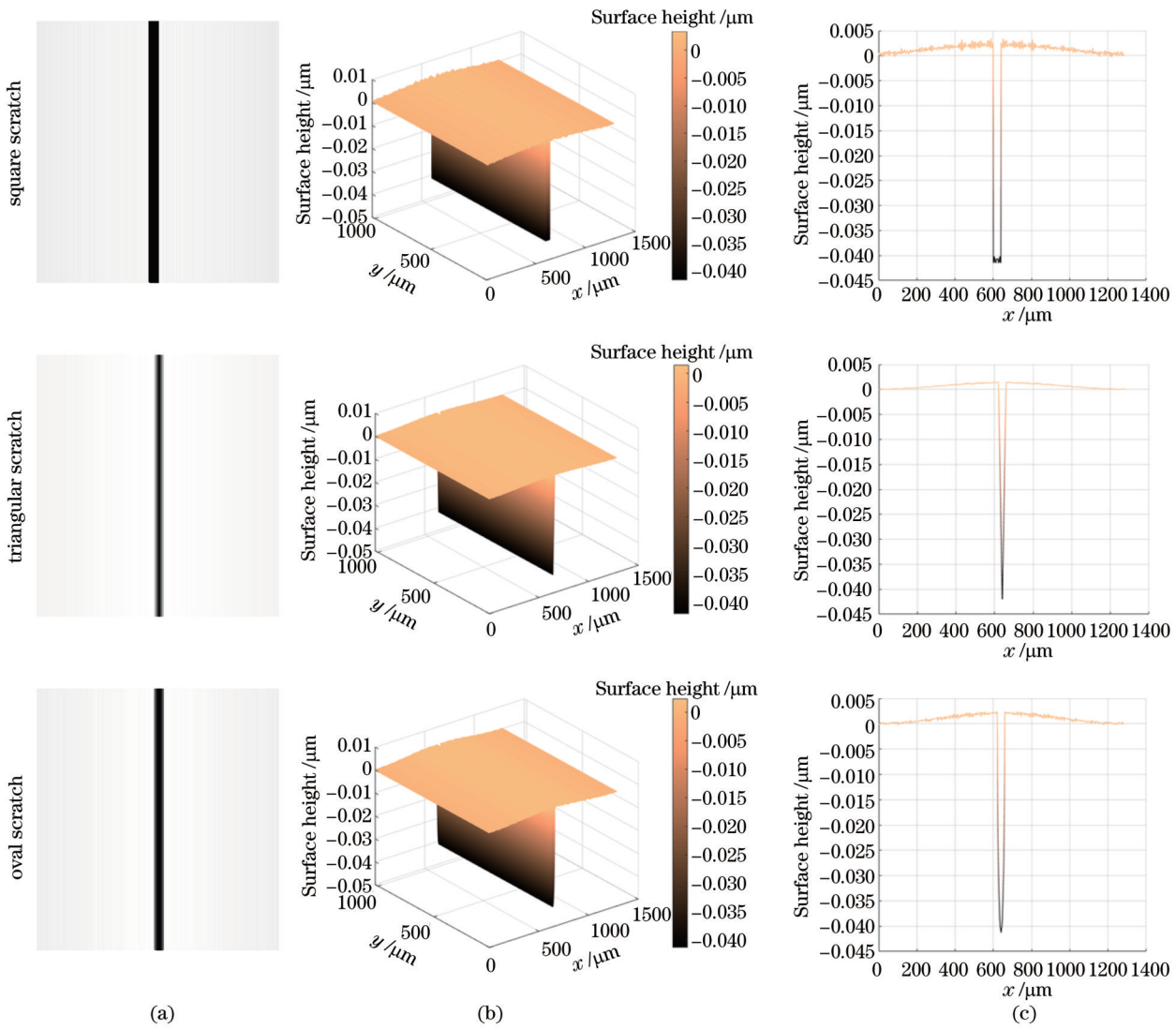


图7 TIE+角谱迭代算法重建结果。(a)横向截面分布;(b)三维分布;(c)纵向截面分布

Fig. 7 Reconstruction results of TIE+angular spectrum iterative algorithm. (a) Transverse cross-section distribution; (b) three-dimensional distribution; (c) longitudinal cross-section distribution

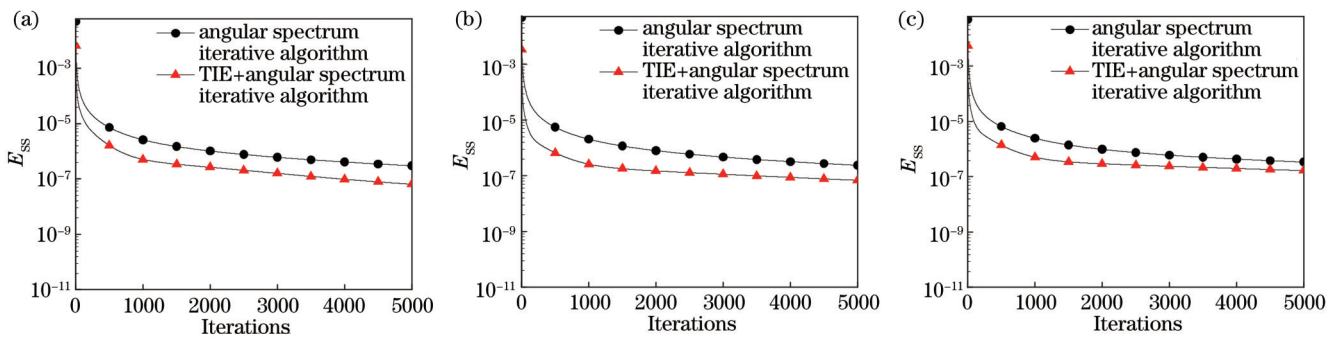


图8 不同类型划痕的强度误差曲线。(a)方形划痕;(b)三角形划痕;(c)椭圆形划痕

Fig. 8 Intensity error curves of different types of scratches. (a) Square scratch; (b) triangular scratch; (c) oval scratch

2) 相关系数评价

为了更好地说明表面划痕深度的重建效果即重建结果的相似程度,采用相关系数对两种算法进行评价,计算公式为

$$\rho(I_{\text{ex}}, I_{\text{out}}) = \frac{1}{L-1} \sum_{i=1}^K \left(\frac{I_i^{\text{ex}} - \mu_{\text{ex}}}{\sigma_{\text{ex}}} \right) \left(\frac{I_i^{\text{out}} - \mu_{\text{out}}}{\sigma_{\text{out}}} \right), \quad (11)$$

式中： I_{ex} 和 I_{out} 分别为重建前后的表面划痕分布图像；
 I_i^{ex} 和 I_i^{out} 分别为 I_{ex} 和 I_{out} 展开成列向量 I^{ex} 和 I^{out} 的第 i

表1 强度误差一定时的迭代次数
Table 1 Iterations when strength error is fixed

Scratch type	Angular spectrum iterative algorithm	TIE+angular spectrum iterative algorithm
Square scratch	3321	953
Triangular scratch	2645	542
Oval scratch	3101	876

个值; L 为展开后列向量的长度; μ_{ex} 和 σ_{ex} 分别为初始划痕图像展开成列向量 I^{ex} 时各元素值的均值和标准差; μ_{out} 和 σ_{out} 分别为重建后划痕图像展开成列向量 I^{out}

时各元素的均值和标准差。当两种算法达到设定的迭代次数(5000次)时,最终重建结果的相关性评价如表2所示。

表2 相关系数计算结果
Table 2 Calculation results of correlation coefficient

Scratch type	Angular spectrum iterative algorithm		TIE+ angular spectrum iterative algorithm	
	Correlation coefficient	Relevance	Correlation coefficient	Relevance
Square scratch	0.9926	Highly relevant	0.9953	Highly relevant
Triangular scratch	0.9901	Highly relevant	0.9947	Highly relevant
Oval scratch	0.9893	Highly relevant	0.9926	Highly relevant

两种重建算法重建结果的相关系数均大于0.9,相关程度都是高度相关,但相对于角谱迭代算法,TIE+角谱迭代算法重建结果的相关系数更大,相关程度更高,重建效果更好。

3) 相对均方根误差评价

采用相对均方根误差来评价两种算法重建划痕深度的准确性。假设计算出的划痕深度为 h_r , 原始划痕深度为 h_0 , 相对均方根误差计算公式为

$$h_{\text{RMS-error}} = \sqrt{\frac{\sum(h_r - h_0)^2}{\sum h_0^2}} \times 100\% \quad (12)$$

设定迭代次数为5000次,计算出不同类型划痕深度的相对均方根误差,计算结果如表3所示。可以看出,两种重建算法的划痕深度相对均方根误差均小于7%,但 TIE+角谱迭代算法相比于角谱迭代算法的相对均方根误差更小,划痕深度重建效果较好。

表3 相对均方根误差计算结果

Table 3 Calculation results of relative root mean square error

unit: %

Scratch type	Angular spectrum iterative algorithm	TIE+angular spectrum iterative algorithm
Square scratch	5.8	5.3
Triangular scratch	6.2	5.2
Oval scratch	6.6	5.3

4 实验研究

4.1 实验装置

根据光学元件表面划痕的散射法检测原理搭建了光场分布图像采集系统,具体实验光路如图9所示。实验中使用的光源是波长为520 nm的半导体激光器;孔径光阑的通光孔大小为Φ10 mm;直角分光棱镜选用的是尺寸为25.0 mm×25.0 mm×25.0 mm,分光比(R/T)为50:50,材料为精退火K9光学玻璃的立方体分光棱镜;CMOS传感器型号是DH-HV1351UM,分辨率为1280 pixel×1024 pixel,像素尺寸为5.2 μm×5.2 μm;透镜的焦距 $f=300.0$ mm;被测元件选择厚度为20 mm、直径为50 mm的圆柱形亚克力材质划痕板,其在可见光范围内的折射率约为1.49,所测划痕的深度范围为10~300 nm,横向尺寸在几微米到几十微米。

实验中,激光器发出的光经过透镜准直后,形成

光束直径较小的平行光,垂直入射到样品表面划痕处,经散射之后的光场分布被CMOS传感器接收。白光干涉仪的划痕检测结果如图10所示,其中 S_a 为表面轮廓高度绝对值的算术平均偏差, S_q 为表面轮廓高度的均方根值, S_z 表示被测元件表面轮廓的最大高度值(最大轮廓峰高与最大轮廓谷深的绝对值之和)。

4.2 划痕深度重建

由于实验过程中会不可避免地引入误差,首先对采集的散射分布图进行中值滤波、直方图均衡化处理,结果如图11所示;然后,分别采用角谱迭代算法、TIE+角谱迭代算法来重建光学元件表面划痕的相位分布;最后,通过式(5)计算得到划痕的深度,重建结果如图12所示。

从图12所示的划痕纵向截面分布图可以看出,其顶部因噪声与初始随机相位影响存在波动,故选取0作为基准面。图12(c)中 h 即为光学元件表面划痕的

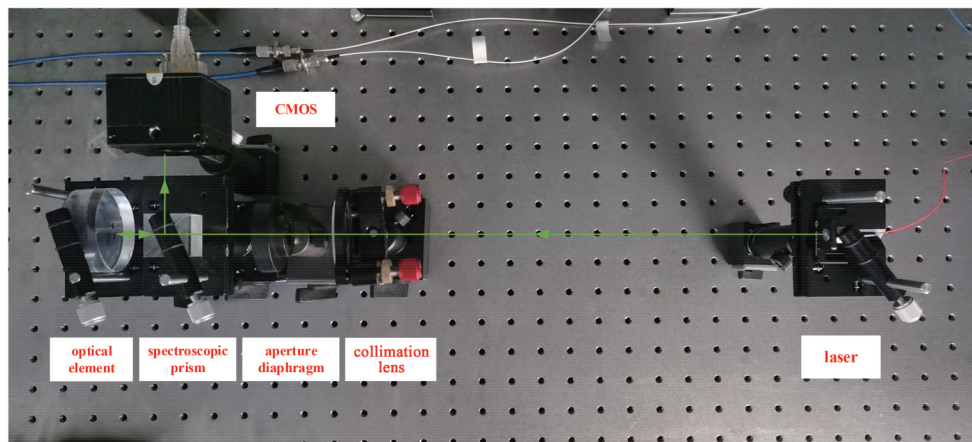


图 9 划痕散射光场分布采集光路

Fig. 9 Scratch scattered light field distribution acquisition optical path

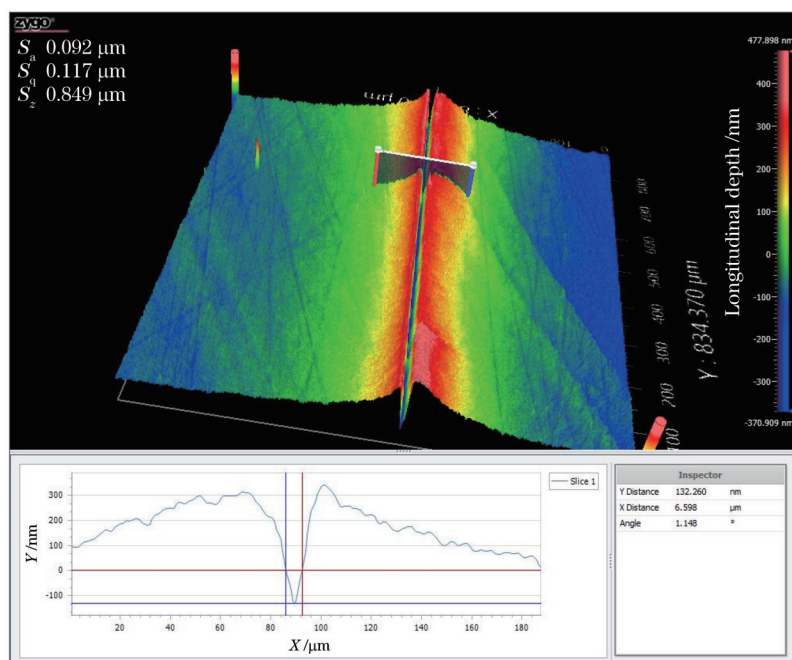


图 10 白光干涉仪检测结果

Fig. 10 Detection result of white light interferometry

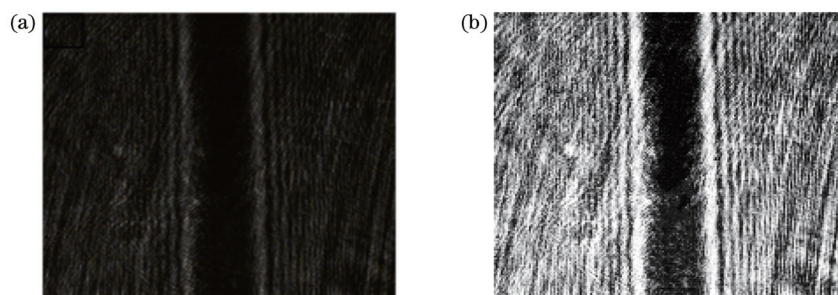


图 11 划痕散射分布。(a) 散射分布;(b) 预处理后的散射分布

Fig. 11 Scattering distribution of scratches. (a) Scattering distribution; (b) scattering distribution after pretreatment

深度,为保证实验结果的准确性,选取 5 处深度测量值求平均值,并将其作为该条划痕深度重建的实际结果。

角谱迭代算法的划痕深度重建结果如表 4 所示,TIE+角谱迭代算法的划痕深度重建结果如表 5 所示。

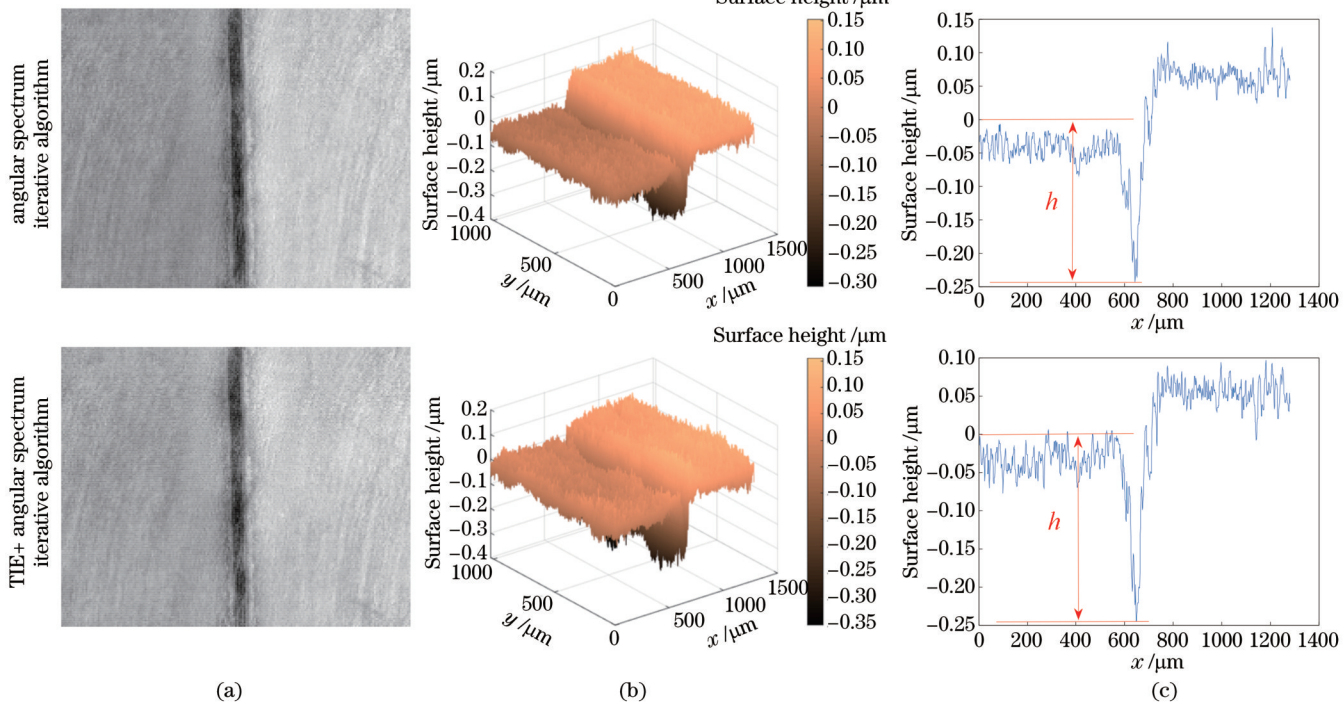


图12 两种算法的划痕深度重建结果。(a)横向截面分布;(b)三维分布;(c)纵向截面分布

Fig. 12 Scratch depth reconstruction results of two algorithms. (a) Transverse cross-section distribution; (b) three-dimensional distribution; (c) longitudinal cross-section distribution

表4 角谱迭代算法对不同深度划痕的重建结果

Table 4 Reconstruction results of scratches with different depths by angular spectrum iterative algorithm unit: \$\mu\text{m}\$

Serial number	Reconstruction value of 5 positions of scratch depth					Average value
	Position 1	Position 2	Position 3	Position 4	Position 5	
1	0.234	0.215	0.194	0.234	0.218	0.219
2	0.219	0.174	0.220	0.224	0.207	0.209
3	0.239	0.213	0.185	0.194	0.193	0.205
4	0.156	0.117	0.131	0.145	0.136	0.137
5	0.134	0.122	0.127	0.136	0.116	0.127

表5 TIE+角谱迭代算法对不同深度划痕的重建结果

Table 5 Reconstruction results of scratches with different depths by TIE+angular spectrum iterative algorithm unit: \$\mu\text{m}\$

Serial number	Reconstruction value of 5 positions of scratch depth					Average value
	Position 1	Position 2	Position 3	Position 4	Position 5	
1	0.243	0.207	0.219	0.215	0.218	0.220
2	0.225	0.214	0.199	0.205	0.217	0.212
3	0.221	0.234	0.229	0.212	0.216	0.224
4	0.134	0.133	0.136	0.152	0.120	0.135
5	0.111	0.139	0.108	0.134	0.124	0.124

4.3 实验分析

使用角谱迭代算法、TIE+角谱迭代算法对采集的光学元件表面光场分布进行重建,得到光学元件表面划痕的深度信息,并将重建结果与白光干涉仪的测量结果进行对比,计算相对误差。两种重建算法重建结果的相对误差如表6所示。

从表6可以看出,角谱迭代算法的相对误差范围为1.35%~4.21%,TIE+角谱迭代算法的相对误差范围为0.90%~3.73%,角谱迭代算法与TIE+角谱迭代算法的相对误差均小于5%,但相较于角谱迭代算法,TIE+角谱迭代算法的相对误差更小,说明TIE+角谱迭代算法对表面划痕深度的重建效果更

表6 两种重建算法相对误差的计算结果
Table 6 Calculation results of relative error of two reconstruction algorithms

Serial number	Depth by white light interferometry / μm	Angular spectrum iterative algorithm		TIE+angular spectrum iterative algorithm	
		Depth / μm	Relative error / %	Depth / μm	Relative error / %
1	0.222	0.219	1.35	0.220	0.90
2	0.218	0.209	4.13	0.212	2.75
3	0.214	0.205	4.21	0.222	3.73
4	0.132	0.137	3.79	0.135	2.27
5	0.125	0.127	1.60	0.123	1.60

好,重建精度更高,重建结果更准确。

5 结 论

将角谱迭代算法与TIE+角谱迭代算法应用到光学元件表面划痕深度检测中。实验过程中只需采集一幅元件表面光场分布图,将其作为重建算法的初始输入来重建划痕的相位信息,再根据表面划痕对相位的调制特性计算出划痕的深度信息。两种重建算法均可以实现对光学元件表面划痕深度的检测,但相较于角谱迭代算法,TIE+角谱迭代算法的重建误差更小,重建精度更高,重建效果更好。

参 考 文 献

- [1] 陆敏,王治乐,高萍萍,等.光学元件的疵病检测及现状[J].光学仪器,2020,42(3): 88-94.
Lu M, Wang Z L, Gao P P, et al. Defect detection and present situation of optical components[J]. Optical Instruments, 2020, 42(3): 88-94.
- [2] 武雄骁,王红军,魏晨,等.基于散射场分布拟合逼近的表面缺陷检测[J].激光与光电子学进展,2021,58(11): 1112003.
Wu X X, Wang H J, Wei C, et al. Surface defect detection based on scattering field distribution fitting approximation[J]. Laser & Optoelectronics Progress, 2021, 58(11): 1112003.
- [3] 向弋川,林有希,任志英.光学元件表面缺陷检测方法研究现状[J].光学仪器,2018,40(1): 78-87.
Xiang Y C, Lin Y X, Ren Z Y. Study on surface defect detection method of optical element[J]. Optical Instruments, 2018, 40(1): 78-87.
- [4] 王维,王杰,黄易杨,等.基于偏振透射结构光的透明物体表面缺陷检测方法[J].光学学报,2021,41(18): 1812002.
Wang W, Wang J, Huang Y Y, et al. Surface defect detection in transparent objects using polarized transmission structured light[J]. Acta Optica Sinica, 2021, 41(18): 1812002.
- [5] 杨飞,高爱华,刘卫国,等.高反射镜表面疵病激光散射显微成像检测[J].电子测量技术,2019,42(4): 110-116.
Yang F, Gao A H, Liu W G, et al. High reflection mirror surface defects of laser scattering imaging detection[J]. Electronic Measurement Technology, 2019, 42(4): 110-116.
- [6] 段珊.光学元件亚表面损伤光散射检测方法研究[D].长春:长春理工大学,2018.
Duan S. Study on light scattering detection method for subsurface damage of optical elements[D]. Changchun: Changchun University of Science and Technology, 2018.
- [7] 张科鹏.基于散射测量的光学元件表面质量评估方法研究[D].北京:中国科学院光电技术研究所,2019.
Zhang K P. Study on surface quality evaluation method of optical elements based on scattering measurement[D]. Beijing: Institute of Optics and Electronics, Chinese Academy of Sciences, 2019.
- [8] 严昆.基于多维复合的相位恢复技术研究[D].杭州:浙江大
- 学,2021.
Yan K. Research on phase recovery technology based on multidimensional composite[D]. Hangzhou: Zhejiang University, 2021.
- [9] Mir M, Bhaduri B, Wang R, et al. Quantitative phase imaging [M]//Progress in optics. Amsterdam: Elsevier, 2012: 133-217.
- [10] 赵彦,高志山,窦健泰,等.一种多波长梯度加速相位恢复迭代算法[J].中国激光,2017,44(1): 0109001.
Zhao Y, Gao Z S, Dou J T, et al. A multi-wavelength gradient acceleration phase retrieval iterative algorithm[J]. Chinese Journal of Lasers, 2017, 44(1): 0109001.
- [11] 吴海燕.非干涉光场的相位恢复算法研究[D].合肥:安徽大学,2012.
Wu H Y. Research on phase recovery algorithm of non-interference light field[D]. Hefei: Anhui University, 2012.
- [12] 张雅彬,陈贤瑞,刘磊,等.基于快速迭代有限差分强度传输方程的相位恢复[J].光学学报,2021,41(22): 2212004.
Zhang Y B, Chen X R, Liu L, et al. Phase retrieval using transport of intensity equation with fast iterative finite difference [J]. Acta Optica Sinica, 2021, 41(22): 2212004.
- [13] 王爱业,潘安,马彩文,等.相位恢复算法:原理、发展与应用[J].红外与激光工程,2022,51(11): 20220402.
Wang A Y, Pan A, Ma C W, et al. Phase recovery algorithm: principle, development and application[J]. Infrared and Laser Engineering, 2022, 51(11): 20220402.
- [14] Gerchberg R, Saxton W O. A practical algorithm for the determination of phase from image and diffraction plane pictures [J]. Optik, 1972, 35: 237-246.
- [15] 杨国桢,顾本源.光学系统中振幅和相位的恢复问题[J].物理学报,1981,30(3): 410-413.
Yang G Z, Gu B Y. On the amplitude-phase retrieval problem in optical systems[J]. Acta Physica Sinica, 1981, 30(3): 410-413.
- [16] Fienup J R. Phase retrieval algorithms: a comparison[J]. Applied Optics, 1982, 21(15): 2758-2769.
- [17] Teague M R. Deterministic phase retrieval: a Green's function solution[J]. Journal of the Optical Society of America A, 1983, 73(11): 1434-1441.
- [18] 刘宏展,纪越峰.一种基于角谱理论的改进型相位恢复迭代算法[J].物理学报,2013,62(11): 114203.
Liu H Z, Ji Y F. An ameliorated fast phase retrieval iterative algorithm based on the angular spectrum theory[J]. Acta Physica Sinica, 2013, 62(11): 114203.
- [19] 梁丽,杨玲,王中科,等.基于TIE和加速角谱迭代算法的二维相位恢复[J].激光与光电子学进展,2013,50(2): 021002.
Liang L, Yang L, Wang Z K, et al. Two-dimensional phase retrieval based on TIE and accelerate angular spectrum iteration algorithm[J]. Laser & Optoelectronics Progress, 2013, 50(2): 021002.
- [20] 程鸿,沈川,张成,等.强度传输方程和角谱迭代融合的相位检索算法[J].中国激光,2014,41(6): 0609001.
Cheng H, Shen C, Zhang C, et al. Phase retrieval algorithm combining transport of intensity equation and angular spectrum iterative[J]. Chinese Journal of Lasers, 2014, 41(6): 0609001.
- [21] 孟春丽,王海凤,刘韵杰,等.基于相位恢复的二维图像彩色

- 再现[J]. 上海理工大学学报, 2019, 41(2): 143-148.
- Meng C L, Wang H F, Liu Y J, et al. Reconstruction of two dimensional color images based on phase retrieval[J]. Journal of University of Shanghai for Science and Technology, 2019, 41 (2): 143-148.
- [22] 于颖, 林大钧, 王海凤. TIE 和 GS 迭代算法用于生物细胞的相位恢复[J]. 光学仪器, 2020, 42(1): 1-6.
- Yu Y, Lin D J, Wang H F. TIE and GS iterative algorithm for phase recovery of biological cells[J]. Optical Instruments, 2020, 42(1): 1-6.
- [23] 潘定中, 刘荣平. 现代数字全息导论: MATLAB 版[M]. 同兴鹏, 严志强, 译. 北京: 机械工业出版社, 2018.
- Poon T C, Liu J P. Introduction to modern digital holography:
- with MATLAB[M]. Yan X P, Yan Z Q, Transl. Beijing: China Machine Press, 2018.
- [24] 郭俊虎. 相干光强恢复相位的方法研究[D]. 武汉: 华中科技大学, 2011.
- Guo J H. Study on the method of recovering phase of coherent light intensity[D]. Wuhan: Huazhong University of Science and Technology, 2011.
- [25] 王金成. 基于强度传输方程的层析重建研究[D]. 合肥: 安徽大学, 2020.
- Wang J C. Study on chromatographic reconstruction based on intensity transmission equation[D]. Hefei: Anhui University, 2020.

Application of TIE and Angular Spectrum Iteration to Scratch Depth Detection on the Surface of Optical Elements

Meng Xin¹, Wang Hongjun^{1*}, Wang Dasen², Tian Ailing¹, Liu Bingcai¹, Zhu Xueliang¹, Liu Weiguo¹

¹Shaanxi Province Key Laboratory of Thin Films Technology and Optical Test, Xi'an Technological University, Xi'an 710021, Shaanxi, China;

²The Ningbo Branch of Ordnance Science Institute of China, Ningbo 310022, Zhejiang, China

Abstract

Objective At present, optical elements are almost always employed in the utilization and development of a wide variety of optical instruments. Due to improper handling during processing, scratches can appear on the surface of optical elements. Scattered light from surface scratches can reduce the beam quality, increase system noise, and reduce contrast, thereby affecting the performance and normal operation of the entire optical system. Therefore, the detection of surface scratches on optical elements is significant. As the existing light scattering methods can only detect the surface scratches of optical elements, the CCD or CMOS sensor can only receive the light field distribution formed by the scattering of surface scratches, from which the two-dimensional size of the surface scratches can be obtained. However, the depth information of the scratches cannot be detected directly. Since up to 80% of the surface information such as depths and shapes of surface scratches is characterized by phase information, we propose to apply the angular spectrum iterative algorithm and transport of intensity equation (TIE) + angular spectrum iterative algorithm to the scattering method for detecting the depth of surface scratches on optical elements. Finally, a scattered light field acquisition optical path is put forward to detect the depths of surface scratches on optical elements.

Methods In the detection of surface scratch depths, the angular spectrum iterative algorithm and transport of intensity equation (TIE) are applied to the detection of surface scratch depths by scattering method. The scratch depths can be obtained from the reconstructed surface scratch phase distribution by the phase modulation characteristics of surface scratches. In the simulation section, the forward and reverse propagation relationship models between the optical element surface and the CMOS receiving surface are built by the angular spectrum transfer function. Based on this model, the scattered light field distributions of surface scratches with different shapes are obtained. Then, the angular spectrum iterative algorithm and TIE+angular spectrum iterative algorithm are adopted to reconstruct the scratch phases. The reconstruction process of the angular spectrum iterative algorithm is to select a random phase as the initial phase of the CMOS receiving surface and iterate repeatedly between the two surfaces. Additionally, the calculated value is replaced with the amplitude value of the initial simulated scattered light field intensity and the unit amplitude of the optical element surface until the defined error reaches the preset precision or the set maximum number of iterations. The phase distribution of scratches on the surface of optical elements can be obtained, and the depths of scratches can be calculated by the modulation characteristics of the surface scratches to the phase. TIE+angular spectrum iterative algorithm is similar to the reconstruction process of the angular spectrum iterative algorithm, which means that the initial random phase is replaced by the phase calculated by TIE. Finally, the effectiveness of the two reconstruction algorithms is evaluated from the strength

error, correlation coefficient, and relative root mean square error. In the experimental section, the scattered light field acquisition device is built and the scattered light field distribution on the surface of the optical element is received by the CMOS detector. At the same time, the reconstructed scratch distribution on the surface of the optical element is reconstructed by the above two reconstruction algorithms, and then the surface scratch depth size is calculated. Finally, the reconstruction results of the two algorithms are compared with the detection results of the white light interferometry, and the relative errors of the two algorithms are calculated.

Results and Discussions In the simulation section, scratch distribution and scattering field distribution of three different shapes, which are square scratch, triangular scratch, and oval scratch, are first simulated (Figs. 4 and 5). Then the scratch scattering field distribution is employed as the initial input of the angular spectrum iterative algorithm and TIE+angular spectrum iterative algorithm respectively to reconstruct the phase distribution of scratches on the surface of optical elements. The depth information of surface scratches is obtained based on the phase modulation characteristics of surface scratches (Figs. 6 and 7). Finally, we evaluate the effectiveness of the two algorithms from the strength error, correlation coefficient, and relative root mean square error. From the perspective of the intensity error evaluation, the number of iterations is set as 5000. The rising number of iterations leads to decreasing intensity error. Compared with the angular spectrum iterative algorithm, TIE+angular spectrum iterative algorithm has a smaller intensity error and faster convergence speed (Fig. 8). From the evaluation of the correlation coefficients, the correlation coefficients of both reconstruction algorithms are greater than 0.9 and the reconstructions are both highly correlated. However, the TIE+angular spectrum iteration algorithm has a greater correlation coefficient and a higher degree of correlation compared to the angular spectrum iteration algorithm. From the evaluation of the relative root mean square error, the relative root mean square error of the TIE+angular spectrum iterative algorithm is 5.2%–5.3%, and that of the angular spectrum iterative algorithm is 5.8%–6.6%. The simulation results show that the scratch depth reconstructed by TIE+angular spectrum iterative algorithm is more accurate. In the experimental section, the scattered light field distribution of scratches on the surface of optical elements is collected experimentally, and the scratch depth on the surface of optical elements is reconstructed through the angular spectrum iterative algorithm and TIE+angular spectrum iterative algorithm (Fig. 12). Finally, the reconstructed results are compared with those of the white light interferometry, and the relative error range of the angular spectrum iterative algorithm is 1.35%–4.21%. The relative error range of the TIE+angular spectrum iterative algorithm is 0.90%–3.73%. The experimental results indicate that the scratch depth reconstructed by TIE+angular spectral iteration algorithm is more accurate.

Conclusions In this paper, we apply the angular spectrum iteration algorithm and TIE+angular spectrum iteration algorithm to the surface scratch depth detection of optical elements by scattering method. During the experiment, only one image of the optical element surface light field distribution needs to be collected, which is employed as the initial input of two reconstruction algorithms to reconstruct the phase information of the scratch. Then the depth information of the scratch is calculated according to the modulation characteristics of the surface scratch to the phase. Compared with the angular spectrum iterative algorithm, TIE+angular spectrum iterative algorithm has a smaller scratch depth reconstruction error, faster convergence speed, higher reconstruction accuracy, and better reconstruction effect.

Key words measurement; scattering method; scattering distribution; scratch depth; phase reconstruction; angular spectrum iterative algorithm; transport of intensity equation